Point-defect calculations for tungsten

R. A. Johnson
Materials Science Department, Thornton Hall, University of Virginia, Charlottesville, Virginia 22901
(Received 6 July 1982)

Computer-model calculations have been carried out for vacancies, divacancies, and interstitials in tungsten using an interatomic potential developed by Johnson and White. Full relaxation of the 531 atoms closest to the defect is carried out by the model, and surrounding atoms are constrained to displace elastically. With an input into the model of a vacancy formation energy of 3.60 eV, the vacancy migration energy, formation volume, and migration volume were 2.00 eV, 0.79Ω, and -0.08Ω, respectively (Ω is the atomic volume). The second-neighbor divacancy was most stable and migrated through partial separation to the fourth neighbor divacancy. The binding energy and volume were 0.78 eV and 0.08Ω, respectively, and migration was similar to that for single vacancies. The potential had to be modified for interstitial calculations to provide repulsion at near separations. For a hard repulsion, the formation energy was large (13.04 eV), the migration energy large (1.05 eV), and the formation volume small (0.13Ω), while for a soft repulsion, the formation and migration energies were smaller (9.30 and 0.20 eV, respectively) and the formation volume was negative (-0.65Ω). Although these calculations do not yield unambiguous results, they suggest that high-temperature curvature in self-diffusion data for tungsten is not caused by divacancies or by single interstitials.

INTRODUCTION

Computer modeling based on two-body interatomic potentials has been used extensively in the study of defects in metals,[1,3] and a number of calculations have been carried out for tungsten. Johnson[4] used the lattice constant and the elastic constants to develop a short-ranged potential (first- and second-neighbor interactions only) and found activation energies of 2.00 and 1.07 eV for vacancy and interstitial migration, respectively. Girifalco and Weizer[5] used the cohesive energy, the lattice constant, and the bulk modulus as physical inputs to determine the three parameters specifying a Morse potential, and this potential has been used by Wynblatt[6] to calculate a vacancy migration energy of 2.26 eV. A potential developed by Johnson and Wilson,[7] based on the lattice constant and the elastic constants as well as the vacancy formation energy, has been used in several calculations: The authors reported a vacancy migration energy of 1.44 eV and divacancy binding at 0.42 eV, while Benedek and Ho[8] used the potential to investigate interstitial formation energies, and Guinan *et al.*[9] found an interstitial migration energy of 0.38 eV with static calculations and 0.365 eV with a dynamic simulation. Benedek and Ho also developed a W potential primarily fitted to phonon dispersion curves, and Stabell and Townsend[10] have given a potential similar to that of Johnson.[6] Johnson and White[11,12] have recently developed a

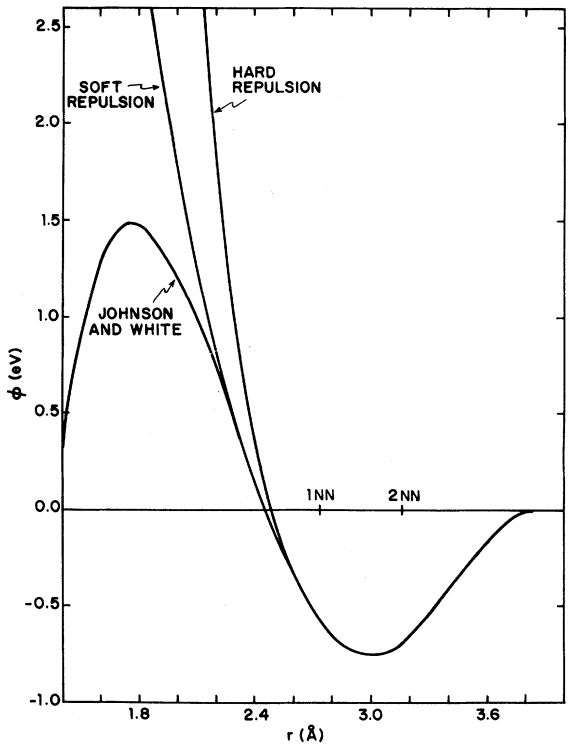

FIG. 1. The potentials used in the calculation. All three give the same vacancy results. The close separation repulsions are required for the interstitial calculations, and the two cases shown are representative of a hard and a soft potential.

short-ranged potential for surface calculations based on the shear elastic constant (but not the bulk modulus), the lattice constant, and the vacancy formation energy, taken as 3.6 eV.[13]

Recent data for W,[14–17] as reviewed by Siegel,[18] yield satisfactory agreement with the result of 3.6 eV for the formation energy and give self-consistent values of 1.8 and 5.4 eV for the migration energy of a vacancy and the low-temperature self-diffusion energy, respectively. A high-temperature activation energy of 6.9 eV is also found[14] which is difficult to explain with a divacancy binding energy of 0.7 eV[17]. The suggestion has been made[16,18] that thermal interstitials are formed at high temperatures and, since they are mobile and might have a larger preexponential factor, could provide an explanation for the high-temperature results.

The primary purpose of the present calculations was to help assess the above interpretation of the data. The Johnson and White potential was chosen because short-ranged potentials have generally proven more successful than long-ranged Morse or Lennard-Jones (Mie) potentials, and the Johnson-Wilson potential had been fitted to a vacancy formation energy of 1.8 eV. The Johnson or the Stabell and Townsend potentials would have given results similar to those reported here.

MODEL

The model and method of calculation are essentially the same as those used earlier.[19] Each atom within a spherical crystallite containing 531 atoms was treated as an independent particle and atoms outside the sphere were constrained as though theory were imbedded in an elastic continuum with radial displacements decreasing as $1/r^2$. Image force corrections were included in the determination of defect volumes. The Johnson and White potential is[12]

$$\phi(r) = -1.26599(r-3.45503)^4 - 3.00836(r-3.45503)^3 + 1.40109(r-3.45503) - 0.34277$$

with r in Å and $\phi(r)$ in eV, is shown in Fig. 1, and is listed in Table I. This potential goes to zero with zero slope midway between second- and third-neighbor separation, and is taken as zero for all larger distances.

VACANCIES AND DIVACANCIES

Vacancy and divacancy results are summarized in Table II. The unrelaxed vacancy formation energy $E_{1V}^{UF}=4.35$ eV was used as an input in the development of the potential. The change in energy due to relaxation was $E_{1V}^{R}=0.75$ eV, yielding a vacancy formation energy of $E_{1V}^{UF}=3.60$ eV. This last value was actually the input because E_{1V}^{UF} was adjusted to reproduce this experimental formation energy. The volume change due to relaxation was $V_{1V}^{R}=-0.21\Omega$ (Ω is the atomic volume), giving a net formation volume of $V_{1V}^{F}=0.79\ \Omega$.

TABLE I. Interatomic potential, with r in Å and ϕ in eV.

Johnson and White: $a=3.16$ Å, $r_c=(1+\sqrt{2})a/2$

$\phi=A(r-r_0)^4+B(r-r_0)^3+C(r-r_0)+D$, $r\le r_c$

$\phi=0$, $r>r_c$

$A=-1.26599$, $B=-3.00836$

$C=1.40109$, $D=-0.34277$

$r_0=3.45503$

Modification for interstitials

$\phi=A\exp[-\alpha(r-r_b)]+B$, $r<r_b$

Hard repulsion

$r_b=r_1=\sqrt{3}a/2$, $\alpha=10.173$

$A=0.371$, $B=-0.942$

Soft repulsion

$r_b=0.925r_1$, $\alpha=4.071$

$A=1.435$, $B=-1.623$

The energy at the vacancy migration midpoint, i.e., with an atom midway between two vacant nearest-neighbor sites, was $E_{1V}^{MP}=5.41$ eV. This configuration was metastable by 0.19 eV with a pair of saddle points for a given migration step about $\frac{1}{3}$ and $\frac{2}{3}$ of the distance along the path of the jumping atom, where it passes through triangular bottlenecks. The resultant migration energy is then $E_{1V}^{M}=2.00$ eV, and the migration volume is small and negative; $V_{1V}^{M}=-0.08\ \Omega$.

The second-neighbor divacancy is by far the most stable with a binding energy of $E_{2V}^{B}=0.78$ eV. First- and third-neighbor binding energies are 0.14 and 0.20 eV, respectively, while third-, fifth-, and sixth-neighbor divacancies are repulsive. The binding volume is small, $V_{2V}^{B}=0.08\ \Omega$, with the second-neighbor configuration, but it is essentially zero for all other arrangements. Defining the unrelaxed divacancy binding energy as the energy of two separated unrelaxed single vacancies minus the energy of an unrelaxed divacancy, $E_{2V}^{UB}=0.57$ and 0.69 eV for first- and second-neighbor configurations, with all others being zero. Thus, the relaxation energy of a first-neighbor divacancy is 0.43 eV less than for two single vacancies, while it is 0.09 and 0.20 eV more for second- and fourth-neighbor divacancies, respectively.

Divacancy migration occurs via a second- to fourth- to second-neighbor process rather than by

TABLE II. Vacancy and divacancy results.

Vacancies: $E_{1V}^{UF}=4.35$ eV

$E_{1V}^{F}=3.60$ eV, $V_{1V}^{F}=0.79\Omega$

$E_{1V}^{M}=2.00$ eV, $V_{1V}^{M}=-0.08\Omega$

Divacancies: $E_{2V}^{UB}(1\text{ NN})=0.57$ eV, $E_{2V}^{UB}(2\text{ NN})=0.69$ eV

$E_{2V}^{B}(1\text{ NN})=0.14$ eV, $V_{2V}^{B}(1\text{ NN})=-0.03\Omega$

$E_{2V}^{B}(2\text{ NN})=0.78$ eV, $V_{2V}^{B}(2\text{ NN})=0.08\Omega$

$E_{2V}^{B}(3\text{ NN})=-0.12$ eV, $V_{2V}^{B}(3\text{ NN})=0.00\Omega$

$E_{2V}^{B}(4\text{ NN})=0.20$ eV, $V_{2V}^{B}(4\text{ NN})=0.01\Omega$

$E_{2V}^{B}(5\text{ NN})=-0.09$ eV, $V_{2V}^{B}(5\text{ NN})=-0.01\Omega$

$E_{2V}^{B}(6\text{ NN})=-0.11$ eV, $V_{2V}^{B}(6\text{ NN})=0.01\Omega$

$E_{2V}^{M}(2\text{-}4\text{-}2)=1.95$ eV $V_{2V}^{M}(2\text{-}4\text{-}2)=-0.08\Omega$

$E_{2V}^{M}(2\text{-}1\text{-}2)=2.50$ eV $V_{2V}^{M}(2\text{-}1\text{-}2)=-0.08\Omega$

second to first to second. The migration energy is $E_{2V}^{M}=1.95$ eV, again with a metastable midpoint configuration, the overall process being very similar to single vacancy migration and having a small negative migration volume: $V_{2V}^{M}=-0.08\ \Omega$. The energy to pass through both triangles is very similar, while, in the second- to first-neighbor jump, the first triangle does not exist due to a missing atom, but the second triangle requires a migration energy of 2.50 eV.

INTERSTITIALS

The potential could not be used for interstitials without modification. It contains no input pertaining to close separations, the curvature becomes negative for $r \lesssim 0.83 r_1$, and the energy becomes negative for small r as shown in Fig. 1. The exponentially repulsive potential

$$\phi = A^{-\alpha(r/r_b-1)} + B$$

was smoothly joined with a matching value, slope, and curvature at $r=r_b$ to the basic potential and was used for $r<r_b$. Two cases, $r_b=r_1$ and $r_b=0.925r_1$, are illustrated in Fig. 1 and are used as examples of a hard and a soft repulsion, respectively. The parameters are listed in Table I. No changes greater than 0.02 eV were found for any of the vacancy results with this modification in the potential.

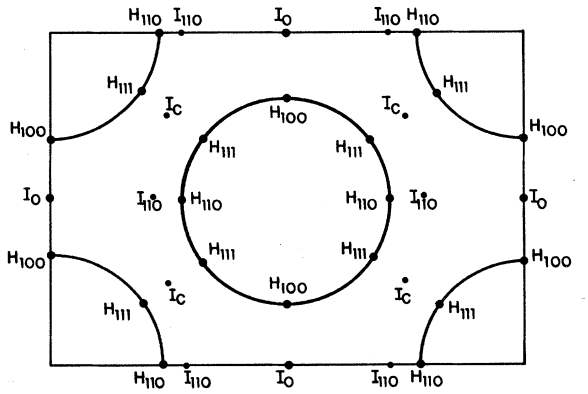

FIG. 2. A {110} plane in the bcc lattice showing interstital configurations. Spheres surrounding each lattice site always contain one atom, with the split configurations consisting of two atoms on opposite sides, each considered half in a sphere. The size of the spheres is appropriate for the soft repulsion case; with hard repulsion the spheres are larger and configurations H_{110} and I_{110} merge.

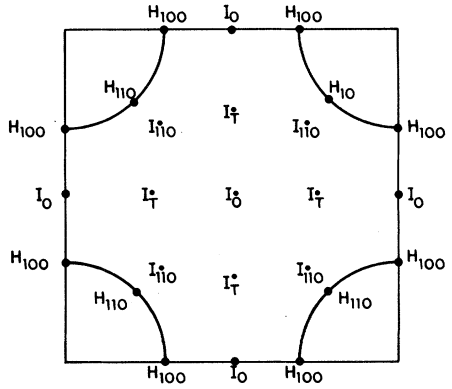

FIG. 3. A {100} plane in the bcc lattice showing interstitial configurations. The notation is the same as for Fig. 2.

TABLE III. Interstitial results.

	E_{1I}^{F} (eV)	$V_{1I}^{F}(\Omega)$	ΔE_{1I}^{F} (min) (eV)
	Hard repulsion: $r_b=r_1$		
H_{110}	13.04	0.13	0
I_s	14.09	0.07	1.05
H_{111}	14.20	−0.01	1.16
I_c	14.28	0.16	1.23
I_T	15.08	−0.21	2.03
I_0	15.35	−0.34	2.31
H_{100}	16.19	−0.35	3.15
	Soft repulsion: $r_b=0.925r_1$		
I_{110}	9.30	−0.65	0
H_{110}	9.43	−0.70	0.13
I_c	9.46	−0.74	0.16
I_s	9.50	−0.66	0.20
H_{111}	9.82	−0.67	0.52
H_{100}	9.85	−0.86	0.55
I_T	9.97	−0.88	0.67
I_0	10.54	−0.87	1.24

The bcc interstitial configurations have been illustrated many times in the literature[19–21] and will not be repeated here. The H configurations contain two atoms symmetrically split about a lattice site I_o, I_t, and I_c are octahedral, tetrahedral, and crowdion configurations, respectively, I_s is the saddle point configuration for interstitial migration, and I_{110} is an additional configuration occurring with the soft repulsion. A (110) plane and a (100) plane are shown in Figs. 2 and 3, respectively, with the circles drawn to scale for the soft repulsion, and the I_{110} location shown. With the harder repulsion, the circles are larger so that H_{110} and I_{110} merge. The saddle point configuration does not occur on a primary plane, and, for example, consists of the jumping atom at $(X,\frac{1}{2},(1-x))(a/2)$ with $x\approx 0.75$.

The basic interstitial results are listed in Table III for both the soft and hard repulsions. For the hard repulsion, $E_{1I}^{F}=13.04$ eV, $V_{1I}^{F}=0.13\Omega$, and $E_{1I}^{M}=1.05$ eV, and for the soft repulsion $E_{1I}^{F}=9.30$ eV, $V_{1I}F$ -0.65Ω, and $E_{1I}^{M}=0.20$ eV. In the latter case, the energy of the I_c configuration is less than that for I_s, but I_c is metastable and the easiest migration path is $I_{110}-I_s-I_{110}$.

DISCUSSION

The vacancy calculations contain no surprises and appear to be consistent with experimental data. The experimental vacancy migration energy is 1.81 eV, while the calculations give 2.00 eV, and there is some field-ion microscopy data giving a divacancy binding energy of 0.7 eV,[17] compared to 0.78 eV from the present work. However, the field-ion microscopy data indicate a stable first-nearest-neighbor divacancy, rather than the second-neighbor configuration strongly favored by the calculations. The data are sparse and apply to a surface under significant strain, not the bulk, so the issue is still open. The activation energy for a divacancy contribution to self-diffusion is $Q_2=E_{2V}^{F}+E_{2V}^{M}=8.37$ eV. Thus, the calculations are in accord with the conclusion that divacancy migration is not the origin of a component of high-temperature self-diffusion with an activation energy of 6.9 eV.[16,18] It is difficult to see how the binding energy could be that much greater and/or migration energy that much less to decrease the calculated Q_2 by 1.47 eV.

The picture emerging from the interstitial calculations is not very clear. Experimentally, with the one interstitial interpretation,[22] interstitials have a very small activation energy in W,[23] which would indicate that a soft potential is appropriate. There are no data for W, but for Mo the interstitial formation volume has been measured as 0.1Ω,[24] in line with present calculations using the hard potential. Also, neither potential is consistent with the $Q=6.9$ eV mentioned above arising from a self-interstitial contribution. Numerous variations were tried for the potential at close separations, but the general pattern showed little change: Any potential hard enough to give $V_{1I}^{F}\approx 0.1\Omega$ also gave a high migration energy, while a soft potential which could give a small migration energy predicted a significant negative formation volume. The energy to break four first-neighbor and three second-neighbor bonds is 4.35 eV, so the energy to insert an interstitial atom into the lattice would have to be about 2.5 eV to yield a $Q=6.9$ eV. An extremely soft potential leading to very close interatomic distances near the interstitial and very little lattice relaxation would be required to obtain this value. Thus, even though the interstitial calculations do not yield unambiguous results, they do provide evidence against an interstitial contribution to self-diffusion. Unfortunately, the present work does not suggest an alternative to self-interstitials or divacancies as an explanation of the curvature in high-temperature diffusion data for W.

ACKNOWLEDGMENT

This work was supported by the National Science Foundation under Grant No. DMR 81-06889.

[1] *Interatomic Potentials and Simulation of Lattice Defects,* edited by P. C. Gehlen, J. R. Beeler, Jr., and R. I. Jaffee (Plenum, New York, 1972).

[2] R. A. Johnson, J. Phys. F 3, 295 (1973).

[3] *Interatomic Potentials and Crystalline Defects,* edited by J. K. Lee (The Metallurgical Society of American Institute of Metallurgical Engineers, New York, 1981).

[4] R. A. Johnson, in *Diffusion in Body-Centered Cubic Metals* (American Society for Metals, Metals Park, Ohio, 1965). p. 357.

[5] L. A. Girifalco and V. G. Weizer, Phys. Rev. 114, 687 (1959).

[6] P. Wynblatt, J. Phys. Chem. Solids 29, 215 (1968).

[7] R. A. Johnson and W. D. Wilson, in *Interatomic Potentials and Simulation of Lattice Defects,* Ref. 1, p. 301.

[8] G. R. Benedek and P. S. Ho, J. Phys. F 4, 183 (1974).

[9] M. W. Guinan, R. N. Stuart, and R. J. Borg, Phys. Rev.

B 15, 699 (1977).
[10]D. E. Stabell and J. R. Townsend, Acta Metall. 22, 473 (1974).
[11]R. A. Johnson and P. J. White, Phys. Rev. B 13, 5293 (1976).
[12]R. A. Johnson and P.J. White, Phys. Rev. B 18, 2939 (1978).
[13]R. J. Gripshover, M. Knoshnevisan, J. S. Zetls, and J. Bass, Philos. Mag. 22, 757 (1970).
[14]J. N. Mundy, S. J. Rothman, N. Q. Lam, and H. A. Hoff, Phys. Rev. B 18, 6566 (1978).
[15]K. Maier, M. Peo, B. Saile, H. E. Schaeffer, and A. Seeger, Philos. Mag. A 40, 701 (1979).
[16]K.-D. Rasch, R. W. Siegel, and H. Schultz, Philos. Mag. A 41, 91 (1980).
[17]J. Y. Park, H.-C. W. Huang, R. W. Siegel, and R. W. Balluffi (unpublished).
[18]R. W. Siegel, in Proceedings of the Yamada Conference V on Point Defects and Point Defect Interactions in Metals, Kyoto, Japan, 1981 (in press).
[19]R. A. Johnson, Phys. Rev. 134, A1329 (1964).
[20]*Fundamental Aspects of Radiation Damage in Metals,* edited by M. T. Robinson and F. W. Young (CONF-751006, 1975), available from the National Technical Information Service, U. S. Department of Commerce, Springfield, Virginia 22161.
[21]*Properties of Atomic Defects in Metals,* edited by N. L. Peterson and R. W. Siegel, (North-Holland, Amsterdam, 1978), reprinted from Nucl. Phys. 69 (1978) and 70 (1978).
[22]See, e.g., W. Schilling, P. Ehrhart, and K. Sonnenberg, in *Fundamental Aspects of Radiation Damage in Metals,* Ref. 20, p. 470; A. Seeger, *ibid.*, p. 493; W. Shilling, *ibid.*, p. 465; W. Frank and A. Seeger, *ibid.*, p. 708.
[23]F. Dausinger and H. Schultz, Phys. Rev. Lett. 35, 1773 (1975).
[24]P. Ehrhart, in *Properties of Atomic Defects in Metals,* Ref. 21, p. 200.